THE JOURNAL OF PHYSICAL CHEMISTRY B LETTERS

2006, *110,* 6454−6457
Published on Web 03/16/2006

Lithium Exchange Processes in the Conduction Network of the Nasicon $LiTi_{2-x}Zr_x(PO_4)_3$ Series ($0 \leq x \leq 2$)

K. Arbi, M. A. París, and J. Sanz*

Instituto de Ciencia de Materiales de Madrid (ICMM), Consejo Superior de Investigaciónes Científicas (CSIC) Cantoblanco, 28049 Madrid, Spain

Received: February 1, 2006; In Final Form: March 2, 2006

Structural sites occupied by lithium in the rhombohedral $LiTi_{2-x}Zr_x(PO_4)_3$ series ($0 \leq x \leq 2$) have been investigated by ^{7}Li NMR spectroscopy. At room temperature, the XRD patterns of the end-members of the series display rhombohedral $R\bar{3}c$ symmetry in $LiTi_2(PO_4)_3$ and triclinic $C\bar{1}$ in $LiZr_2(PO_4)_3$. In the first compound, Li ions occupy M1 sites; however, in the second one Li occupy intermediate $M_{1/2}$ sites. As the temperature increases, a first-order displacive transformation is detected in the triclinic phase, but a second-order/disorder transition is detected in the rhombohedral phase. From the temperature dependence of the ^{7}Li NMR quadrupole constant (C_Q) of the two compounds, the evolution of M_1 and $M_{1/2}$ sites occupancy in the Nasicon conduction network has been deduced. At high temperatures, analyzed phases tend toward a disordered rhombohedral phase, in which both M_1 and $M_{1/2}$ sites are equally populated and in which lithium mobility is favored by the existence of vacant M_1 sites. According to this study, this phase can also be obtained by substituting Ti by Zr in the $LiTi_{2-x}Zr_x(PO_4)_3$ series.

Introduction

Interest in lithium ion conducting solids has considerably increased because of their potential application as electrolytes in rechargeable lithium batteries. $LiM^{IV}_2(PO_4)_3$ compounds with NASICON[1] structure (acronym for Na SuperIonic Conductors) have been extensively studied for their good ionic conductivity.[2−6] In these compounds, structure is formed by $M_2(PO_4)_3$ units in which each MO_6 octahedron shares corners with six PO_4 tetrahedra and each tetrahedron shares oxygens with four octahedra (Figure 1a). The ideal framework displays the rhombohedral symmetry (space group $R\bar{3}c$), but in some particular cases a triclinic distortion (space group $C\bar{1}$) has been detected.[7−9] In the rhombohedral $LiM^{IV}_2(PO_4)_3$ phases (M^{IV} = Ge and Ti), Li ions occupy M_1 sites at trigonal *c*-axes, with a six-fold oxygen coordination. However, in triclinic phases (M^{IV} = Sn, Hf, Zr) Li ions are four-fold coordinated at intermediate $M_{1/2}$ positions between M_1 and M_2 sites (Figure 1a). Triclinic $LiM^{IV}_2(PO_4)_3$ compounds exhibit a triclinic-rhombohedral transition that has been analyzed by neutron diffraction.[7−10]

In general, Li conductivity is higher and activation energy lower in rhombohedral phases. In these samples, activation energies for lithium motion decreases when the size of tetravalent M cations increases.[6] In the present work, ^{7}Li NMR spectroscopy has been used to analyze occupation of structural sites and mobility of lithium in the fast ion conductor series $LiTi_{2-x}Zr_x$ $(PO_4)_3$ ($0 \leq x \leq 2$). In these compounds, the substitution of Ti by Zr expands the rhombohedral unit cell (see Table 1); however, information concerning the Li-sites occupation is not available.

* To whom correspondence should be addressed. E-mail: jsanz@icmm.csic.es.

Experimental Section

$LiTi_{2-x}Zr_x(PO_4)_3$ compounds ($0 \leq x \leq 2$) have been prepared following the method described elsewhere.[11,12] X-ray diffraction (XRD) was used to assess purity of prepared compositions. XRD patterns were recorded with the Cu Kα radiation ($\lambda = 1.5405981$ Å) in the temperature range 25−500 °C, using a high-temperature AP HTK10 camera adapted to a PW 1050/25 Phillips diffractometer. Powder XRD patterns were collected in the 10−70° 2θ range with a step size of 0.02° and a counting time of 0.1 s/step. The Fullprof program was used to determine unit cell parameters of prepared samples.

^{7}Li MAS NMR spectra were recorded in a MSL-400 Bruker spectrometer (9.4 T) at 155.50 MHz. Spectra were obtained after $\pi/2$ pulse irradiation ($\approx 4\ \mu$s) with a recycling time of 10 s. The number of scans was 400. In the temperature range 100−450 K, quadrupole interactions remain small (C_Q < 180 kHz), making the irradiation of the central and satellite transitions non selective. ^{7}Li NMR chemical shifts were given relative to a 1 M LiCl aqueous solution. The fitting of the NMR spectra was carried out with the Bruker WINFIT software package.[13] This program allows the position, line width and intensity of components to be determined; however, quadrupole C_Q and η values have to be deduced with a trial and error procedure.

Results and Discussion

XRD patterns of the $LiTi_{2-x}Zr_x$ $(PO_4)_3$ ($0 \leq x \leq 2$) series are given in Figure 2. In this figure, a progressive shift of diffraction peaks to lower 2θ values is observed that corresponds to the unit cell expansion induced by Zr for Ti substitution. The progressive increase of the c/a ratio produces the splitting

10.1021/jp060677u CCC: $33.50

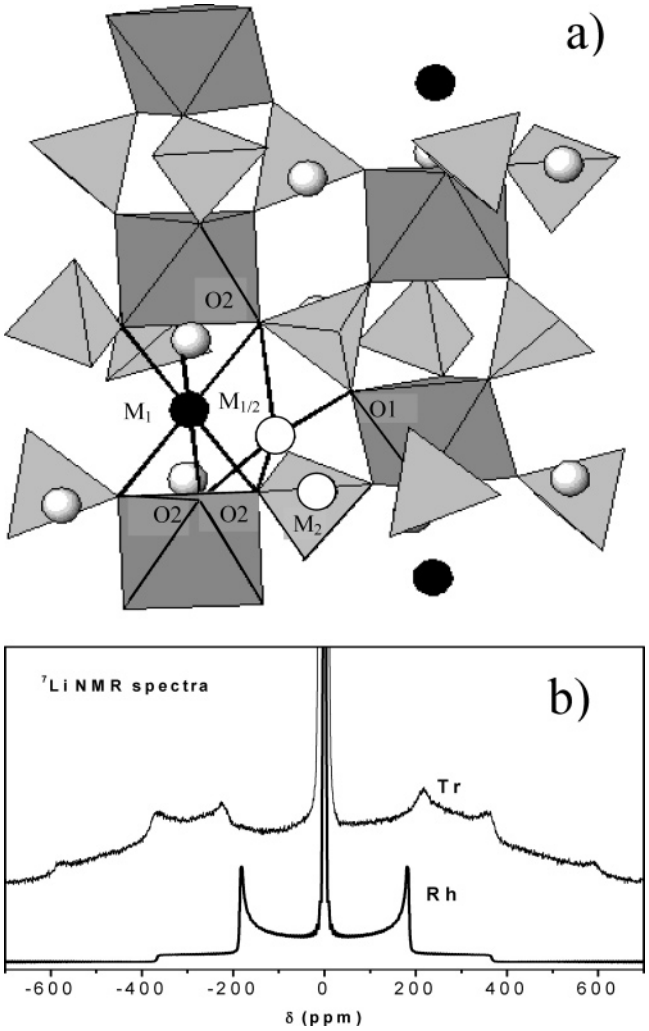

Figure 1. (a) Rhombohedral structure of Nasicon compounds showing structural M_1, $M_{1/2}$, and M_2 sites. (b) Static ^{7}Li NMR spectra of triclinic and rhombohedral $LiZr_2(PO_4)_3$ phases.

TABLE 1: Quadrupole Constant, C_Q (kHz), Asymmetry Parameter, η, and Hexagonal Unit Cell Parameters of the Rhombohedral $LiTi_{2-x}Zr_x(PO_4)_3$ Series

x_{Zr}	C_Q (KHz)	η (dimensionless)	a (Å)	c (Å)
0	44	0	8.511	20.843
0.4	50	0	8.566	21.071
0.63	65	0	8.605	21.212
1	73,3	0	8.672	21.462
1.5	88	0	8.764	21.779
2	100,5	0	8.847	22.241

of (104) and (110) peaks near 20°, and that of the (214) and (300) peaks near 36.5°. Unit cell parameters deduced from these patterns are given in Table 1. In the case of the sample $x = 2$, only the XRD pattern of the rhombohedral phase, recorded at 70 °C, has been considered.

^{7}Li NMR ($I = 3/2$) spectra of the $LiR_2(PO_4)_3$ samples are formed by a central ($-1/2,1/2$) and two satellite ($-3/2,-1/2$ and $1/2,3/2$) transitions.[14] In previous works, quadrupole constants (C_Q and η parameters) of lithium located at M_1 and $M_{1/2}$ sites were deduced in $LiM^{IV}_2(PO_4)_3$ compounds.[15,16] In $LiZr_2(PO_4)_3$ samples, satellite lines of the triclinic phase are split over a larger region than in the rhombohedral phase (see Figure 1b). From analysis of ^{7}Li NMR spectra, quadrupole C_Q and η constants of the $LiTi_{2-x}Zr_x(PO_4)_3$ series have been deduced (see Table 1).

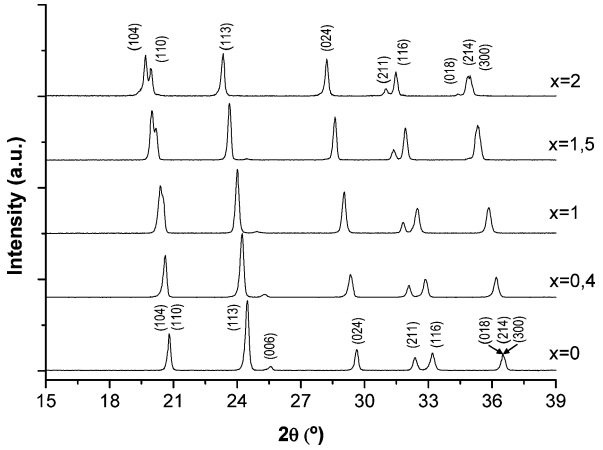

Figure 2. XRD patterns of the series Li $Ti_{2-x}Zr_x(PO_4)_3$ recorded at room temperature. The XRD pattern of the sample with $x = 2$ corresponds to that of the rhombohedral phase recorded at 70 °C.

In previous works, quadrupole C_Q and η_Q constants were calculated with expressions[15,16]

$$C_Q = \frac{e^2 Q V_{zz}}{h} \qquad \eta_Q = \frac{V_{xx} - V_{yy}}{V_{zz}} \tag{1}$$

where Q is the quadrupole moment of nuclei and V_{xx}, V_{yy}, V_{zz} are the principal values of the electric field gradient (EFG) tensor at structural sites occupied by lithium. In the triclinic $LiZr_2(PO_4)_3$ phase, quadrupole constants calculated for $M_{1/2}$ sites, $C_Q = 180$ kHz and $\eta_Q = 0.6$, are similar to those deduced from NMR spectra recorded at 300 K.[11] At these sites, lithium exhibits an almost planar four-fold coordination with Li−O distances between 1.9 and 2.26 Å.[9] In the rhombohedral $LiTi_2(PO_4)_3$ phase, the experimental $C_Q = 35$ kHz deduced from NMR spectra at 300 K corresponds to that calculated for lithium at M_1 sites, with Li−O distances near 2.1 Å.[12,17] In the rhombohedral $LiZr_2(PO_4)_3$ sample, mean Li−O distances should increase above 2.40 Å in M_1 sites; however, Li ions move to six positions related by -3 symmetry axes in order to reduce Li−O distances to 2.3 Å in M_1 cavities.[10] In this phase, the analysis of quadrupole constants was difficult because of the Li hopping between equivalent sites.

The mobility of lithium produces the partial average at the NMR time scale ($t \sim 10^{-8}$ s) of quadrupole C_Q constants of occupied sites. From this fact, the temperature dependence of the quadrupole C_Q constant can inform us about the relative occupation of M_1 and $M_{1/2}$ sites. The variations of C_Q values of $LiTi_2(PO_4)_3$ and $LiZr_2(PO_4)_3$ are given in Figure 3a. For sake of comparison, C_Q values measured in isostructural $LiGe_2(PO_4)_3$ and $LiHf_2(PO_4)_3$ phases are also included. In triclinic $LiZr_2(PO_4)_3$ and $LiHf_2(PO_4)_3$ phases, C_Q and η values are more important (180 kHz, 0.6), indicating that sites occupied by Li display lower symmetry. Along the triclinic−rhombohedral transformation (displacive first-order transition), significant changes were detected in geometry and disposition of ZrO_6 and PO_4 polyhedra, that produced the decrease on C_Q to 120 kHz and η to 0. In the rhombohedral $LiTi_2(PO_4)_3$ sample, C_Q is nearly constant (~20 kHz) below 250 K, but increases up to 70 kHz at 500 K, indicating that occupation of Li sites changes (second-order transition). In the rhombohedral $LiTi_{2-x}Zr_x(PO_4)_3$ series, quadrupole C_Q constants measured at room temperature increase from 40 to 120 kHz as the Zr content increases (Figure 3b). In samples with $x > 1.5$, quadrupole constants measured at room temperature are near those measured at 340 K in the rhombohedral $LiZr_2(PO_4)_3$ phase.[11]

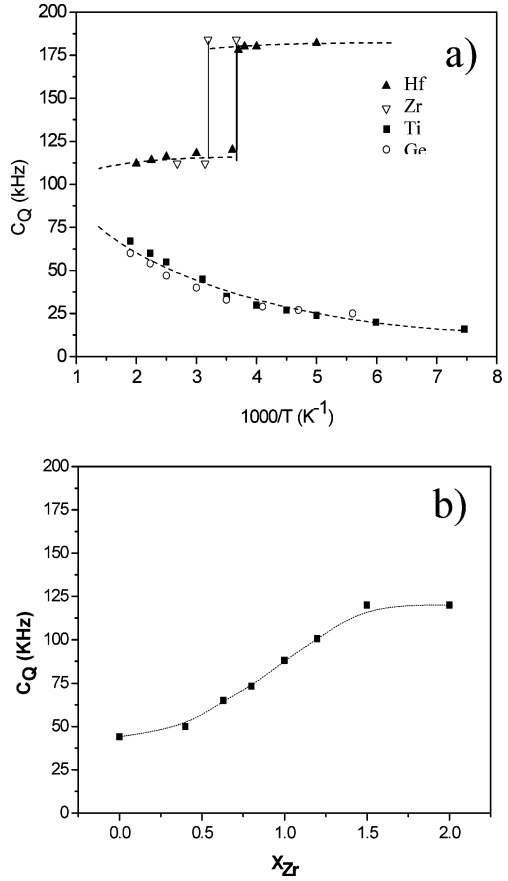

Figure 3. (a) Temperature dependence of quadrupole C_Q constants deduced from ^{7}Li NMR spectra of the $LiR_2(PO_4)_3$ series, R = Ge, Ti, Zr, and Hf. (b) Dependence of the quadrupole C_Q constant on the composition of the $LiTi_{2-x}Zr_x(PO_4)_3$ series. ^{7}Li NMR spectra were recorded at room temperature. In the case of $x = 2$, the CQ value corresponds to the sample heated at 70 °C.

To investigate factors limiting the lithium mobility, we have analyzed the geometry of triangular bottlenecks T_1 ($O_2O_2O_1$) and T_2 ($O_2O_2O_2$) located between M_1 and M_2 sites (see Figure 1a). In this analysis, we have determined Li−O distances necessary to pass Li ions through the windows (radius of inscribed spheres). In the triclinic $LiZr_2(PO_4)_3$ phase, Li−O distances at T1 (four sided) and T2 (three sided polygones) windows are near 2.06 and 2.25 Å; however, these distances become 2.20 and 2.18 Å in the rhombohedral $LiZr_2(PO_4)_3$ phase. In the rhombohedral $LiTi_2(PO_4)_3$ phase, Li−O distances at T1 and T2 windows are near 2.05 and 1.98 Å. According to this analysis, T2 windows limit Li mobility in rhombohedral $LiTi_2(PO_4)_3$, but T1 windows limit lithium diffusion in the triclinic $LiZr_2(PO_4)_3$ phase.

Fast Exchange Processes. At increasing temperatures, T1 and T2 windows expand favoring Li mobility in the conduction network. In this case, fast exchange processes between M_1 and $M_{1/2}$ sites should produce a signal with intermediate characteristics. According to this model, the monotonic increment of C_Q detected in $LiTi_2(PO_4)_3$ has been interpreted by assuming that the residence time at $M_{1/2}$ sites (probability $P_{1/2}$) increases at the expense of that at M_1 sites (probability P_1).[12] This increment can be analyzed with the expression[15,16]

$$C_Q = \frac{C_Q{}^1 P_1 + C_Q{}^2 3P_{1/2}}{P_1 + 3P_{1/2}} \qquad (2)$$

where, $C_Q{}^1 = 15$ and $C_Q{}^2 = 170$ kHz are the quadrupole constants and P_1 and $P_{1/2}$ are the occupation probabilities of M_1 and $M_{1/2}$ sites by lithium. The factor 3 takes into account the multiplicity of $M_{1/2}$ sites with respect to M_1 sites.

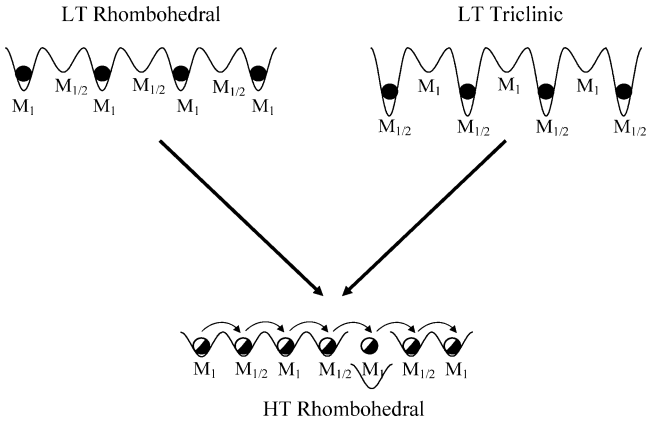

Figure 4. Variation of energy barriers produced during the heating of the rhombohedral and triclinic end members of the $LiTi_{2-x}Zr_x(PO_4)_3$ series.

Extended Li motions are favored by creation of vacant M_1 sites at the intersection of conduction channels in rhombohedral phases. From the analysis of C_Q values, it was shown that creation of vacancies at M_1 sites is an activated process, with an E_a near 0.07 eV.[18] However, C_Q values measured at 450 K showed that 2/3 of M_1 sites are still occupied at this temperature. From this fact, the total vacancy disordering, $P_1 = P_2 = 0.25$ ($C_Q \approx 100$ kHz) is not attained in $LiTi_2(PO_4)_3$, in the temperature range 200−500 K.

In the triclinic $LiZr_2(PO_4)_3$ phase, Li ions occupy $M_{1/2}$ sites, but in the rhombohedral $LiZr_2(PO_4)_3$ phase, T1 and T2 windows cannot coordinate Li ions, favoring Li mobility.[10,11,19] At the triclinic-rhombohedral transition, the quadrupole constant C_Q decreased from 180 to 120 kHz and η from 0.6 to 0. In this case, the full exchange between M_1 and $M_{1/2}$ sites, $P_1 = P_2 = 0.25$ ($C_Q \approx 100$ kHz), reproduces reasonably well experimental results. Fast exchange processes between M_1 and $M_{1/2}$ sites, simulates also the rhombohedral $R\bar{3}c$ symmetry ($\eta_Q = 0$). This model differs from that deduced from diffraction experiments, where occupation of intermediate $M_{1/2}$ sites was not analyzed in the rhombohedral $LiZr_2(PO_4)_3$ phase.[20]

At this point, it is interesting to analyze Li mobility in the $LiTi_{2-x}Zr_x(PO_4)_3$ series. In the rhombohedral $LiTi_2(PO_4)_3$ end-member, Li ions occupy M_1 sites and activation energy for Li motion, E_a, is 0.46 eV. In the triclinic $LiZr_2(PO_4)_3$ phase, Li ions occupy $M_{1/2}$ sites and activation energy E_a is 0.6 eV. Finally, occupation of M_1 and $M_{1/2}$ sites becomes similar and activation energy for Li motion decreased to 0.3 eV in the rhombohedral $LiZr_2(PO_4)_3$ phase (see Figure 4). A similar effect can be obtained by substitution of Ti by Zr in $LiTi_{2-x}Zr_x(PO_4)_3$ series. In these samples, unit cell expansion associated with Zr incorporation favors the progressive occupation of $M_{1/2}$ at the expense of M_1 sites. Along this series, Li mobility increases and activation energy E_a decreases from 0.46 to 0.3 eV[2]. The stabilization of the rhombohedral phase in Zr-doped samples eliminates problems derived from stresses produced at the triclinic−rhombohedral transition and enlarges the electrochemical window (lower reducibility of Zr) of experimental devices.

Conclusions

Li sites and lithium mobility in $LiTi_{2-x}Zr_x(PO_4)_3$ series have been analyzed with ^{7}Li NMR spectroscopy. From the analysis of quadrupole constants of end members of the series, the

preferential occupation of M_1 sites in rhombohedral and that of $M_{1/2}$ sites in triclinic phases were deduced.

The analysis of the temperature dependence of C_Q values showed the progressive occupation of midway $M_{1/2}$ sites at the expense of M_1 sites when the temperature increases in the rhombohedral $LiTi_2(PO_4)_3$ sample. The opposite effect was detected in triclinic $LiZr_2(PO_4)_3$ samples, where $M_{1/2}$ sites are preferentially occupied at low temperatures. Above the triclinic−rhombohedral transition, a full delocation of lithium on M_1 and $M_{1/2}$ sites was detected. In the case of $LiTi_{2-x}Zr_x(PO_4)_3$ series, a similar effect is produced when Ti is substituted by larger Zr cations. The stabilization of the rhombohedral phase in Zr-doped samples eliminates problems derived from stresses produced at the triclinic−rhombohedral transition and enlarges the electrochemical window (lower reducibility of Zr) of experimental devices.

Acknowledgment. This work was supported by the Spanish CICyT Agency (projects MAT2001-3713 and MAT2004-3070). K.A. thanks Spanish Ministry of Science and Technology for financial support.

References and Notes

(1) Goudenough, J. B.; Hong, H. Y.-P.; Kafalas, J. A. *Mater. Res. Bull.* **1976**, *11*, 203.

(2) Winand, J. M.; Rulmont, A.; Tarte, P. *J. Solid State Chem.* **1991**, *93*, 341.

(3) Martinez-Juárez, A.; Rojo, J. M.; Iglesias, J. E.; Sanz, J. *Chem. Mater.* **1995**, *7*, 1857.

(4) Sudreau, F.; Petit, D.; Boilot, J. P. *J. Solid State Chem.* **1989**, *83*, 78.

(5) París, M. A.; Martínez-Juárez, A.; Iglesias, J. E.; Rojo, J. M.; Sanz, J. *Chem. Mater.* **1997**, *9*, 1430.

(6) Martinez-Juárez, A.; Pecharromán, C.; Iglesias, J. E.; Rojo, J. M. *J. Phys. Chem. B* **1998**, 102, 372.

(7) Morin, E.; Angenault, J.; Couturier, J. C.; Quarton, M.; He, H.; Klinowski, J. *Eur. J. Solid State Inorg. Chem.* **1997**, *34*, 947.

(8) Losilla, E. R.; Aranda, M. A. G.; Martinez-Lara, M.; Bruque, S. *Chem. Mater.* **1997**, *9*, 1678.

(9) Catti, M.; Stramare, S.; Ibberson, R. *Solid State Ionics* **1999**, *123*, 173.

(10) Catti, M.; Starmare, S. *Solid State Ionics* **2000**, *136*−*137*, 489.

(11) Arbi, K.; Lazarraga, M. G.; Chehimi, D. B.; Ayadi-Trabelsi, M.; Rojo, J. M.; Sanz, J. *Chem. Mater.* **2004**, *16*, 255.

(12) París, M. A.; Martinez-Juárez, A.; Rojo, J. M.; Sanz, J. *J. Phys. Condens. Matter* **1996**, *8*, 5355.

(13) Massiot, D. *WINFIT; Bruker-Franzen Analytik GmbH;* Bremen: Germany, 1993.

(14) Abragam, A. *The Principles of Nuclear Magnetic*; Oxford University Press: Oxford, 1961.

(15) París, M. A.; Sanz, J. *Phys. Rev. B* **1997**, *55*, 14270.

(16) París, M. A.; Sanz, J. *Phys. Rev. B* **2000**, *62*, 810.

(17) Aatiq, A.; Ménétrier, M.; Croguennec, L.; Suard, E.; Delmas, C. *J. Mater. Chem.* **2002**, *12*, 2971.

(18) Arbi, K.; Tabellout, M.; Lazarraga, M. G.; Rojo, J. M.; Sanz, J. *Phys. Rev. B* **2005**, *72*, 094302.

(19) Sudreau, F.; Petit, D.; Boilot, J. P. *J. Solid State Chem.* **1989**, *83*, 78.

(20) Catti, M.; Stramare, S. *Chem. Mater.* **2003**, *15*, 1628.